Journal of the American College of Cardiology
© 2009 by the American College of Cardiology Foundation
Published by Elsevier Inc.

Vol. 53, No. 14, 2009
ISSN 0735-1097/09/$36.00
doi:10.1016/j.jacc.2008.10.064

PRE-CLINICAL RESEARCH

Cardiac Deletion of the Coxsackievirus-Adenovirus Receptor Abolishes Coxsackievirus B3 Infection and Prevents Myocarditis In Vivo

Yu Shi, MD, PHD,* Chen Chen, MSC,* Ulrike Lisewski, MSC,* Uta Wrackmeyer, MSC,* Michael Radke, PHD,* Dirk Westermann, MD,† Martina Sauter, DVM,‡ Carsten Tschöpe, MD,† Wolfgang Poller, MD,† Karin Klingel, MD,‡ Michael Gotthardt, MD*§

Berlin and Tübingen, Germany; and Pullman, Washington

Objectives We investigated the role of the Coxsackievirus-adenovirus receptor (CAR) in viral myocarditis.

Background CAR is involved in virus uptake into various cell types. It has therefore been suggested as a therapeutic target to prevent or treat Coxsackievirus B3 (CVB3)-induced diseases such as myocarditis and cardiomyopathy. Recent work in CAR-deficient animals has indicated a role in embryonic development and remodeling with cardiac malformation and lethality.

Methods We generated a tamoxifen-inducible knockout (KO) mouse to study CAR in the adult heart after CVB3 infection. Histomorphology, virus distribution, and cardiac function were compared in CAR-KO versus noninduced littermate control animals expressing wild-type CAR (WT).

Results We have demonstrated that eliminating CAR prevents signs of inflammatory cardiomyopathy, with essentially no pathology in KO hearts. Unlike CVB3-infected WT control animals, the cardiac inducible KO mice did not exhibit structural changes such as monocyte infiltration or fibrosis after CVB3 infection or increased production of markers of inflammation such as interleukin-6 and -10. Whereas CVB3 infection resulted in severe contractile dysfunction in the hearts of animals that express WT, the CAR-deficient hearts appeared normal.

Conclusions Elimination of CAR in adult hearts can efficiently block virus entry and the associated pathology including contractile dysfunction. The lack of infiltration or other morphological changes in CVB3-infected KO hearts emphasizes the contribution of direct virus-mediated pathology in enteroviral myocarditis. (J Am Coll Cardiol 2009; 53:1219–26) © 2009 by the American College of Cardiology Foundation

Coxsackievirus B3 (CVB3) infections are frequent causes of human acute myocarditis, often resulting in chronic cardiomyopathy with fibrosis and reduced contractile function that might progress into terminal heart failure. The cellular receptors of CVB3 are the Coxsackievirus-adenovirus receptor (CAR) and the decay-accelerating factor (DAF)/CD55 (1–4). CAR is a 46 kD type I transmembrane protein of the tight junction and intercalated discs, where it mediates homotypic cell adhesion through its extracellular Ig-domains (5). The cytoplasmic tail is alternatively spliced and interacts with various adaptor proteins that link to signal transduction and endocytosis (5–8). CAR is expressed in a variety of tissues, including the heart, brain, and pancreas (1,2,9). It is highly regulated in the developing heart and significantly reduced after birth, which suggests a role in remodeling of the embryonic heart (9). Various CAR-deficient animal models have been generated to gain additional insight into its physiological functions (10–12). Targeting either exon 1 or 2 results in cardiac malformation, degeneration, and lethality in mid-gestation of the conventional knockouts (KOs). These phenotypes indicate a role for CAR in morphogenesis and differentiation of the heart. In addition to providing a genetic tool to generate loss of function mutants, the mouse is also a suitable animal model to study the role of CAR in CVB3-induced pancreatitis and myocarditis, because pathomechanisms and disease progres-

See page 1227

From *Neuromuscular and Cardiovascular Cell Biology, Max-Delbrück-Center for Molecular Medicine, Berlin, Germany; †Department of Cardiology, Charité–Campus Benjamin Franklin, Berlin, Germany; ‡Department of Molecular Pathology, University Hospital Tübingen, Tübingen, Germany; and the §Department of Veterinary and Comparative Anatomy, Pharmacology, and Physiology, Washington State University, Pullman, Washington. This study was supported by the DFG SFB TR19. Dr. Shi and Miss Chen contributed equally to this work.

Manuscript received July 30, 2008; revised manuscript received September 16, 2008, accepted October 7, 2008.

Abbreviations and Acronyms

CAR = Coxsackievirus-adenovirus receptor
CVB3 = Coxsackievirus B3
DAF = decay-accelerating factor
FAM = carboxyfluorescein
IL = interleukin
INF = interferon
KO = knockout
LCK = lymphocyte protein tyrosine kinase
LV = left ventricle/ventricular
MCM = MerCreMer transgenic
p.i. = after injection with virus
TAMRA = carboxy-tetramethy-lrhodamine
TNF = tumor necrosis factor
WT = noninduced littermate control animals expressing wild-type Coxsackievirus-adenovirus receptor

sion are similar in human patients and mice (13,14). The objective of this study is to investigate the role of CAR in viral myocarditis. Elimination of CAR in the adult heart can abolish cardiac CVB3 infection and prevent the evolvement of myocarditis and consequently of fibrosis and reduced contractile function.

Methods

Generation of inducible CAR-KO mice. To generate CAR-deficient animals we assembled a targeting construct flanking CAR exon 1, which contains the ATG, with lox sites (Fig. 1A). This strategy precludes expression of both the membrane-bound and soluble CAR isoforms. After homologous recombination, blastocyst injection of embryonic stem cells was used to obtain KO animals. The neomycine/flp resistance cassette was removed by germline expression of the FLP recombinase (15). The resulting animals were verified by polymerase chain reaction and Southern blot (Figs. 1B and 1C) and maintained on a mixed 129SVJ/C57black6 background breeding MerCreMer transgenic $(MCM)^+$ (16) $CAR^{(RECf/RECf)}$ floxed animals to MCM^- $CAR^{(RECf/RECf)}$ animals. This approach yields 50% littermate control subjects that express wild-type CAR (WT). Tamoxifen in peanut-oil (10 $\mu g/\mu l$) was injected into animals at 2 months of age. Five injections/week for 2 consecutive weeks (10 injections; 300 mg/kg total) resulted in a >10-fold difference in CAR expression levels after 3 months (Fig. 1D). All experiments involving animals were carried out following institutional and National Institutes of Health guidelines, "Using Animals in Intramural Research."

Virus and mice. Complementary deoxyribonucleic acid-generated CVB3 Nancy strain (17) was grown and propagated in Vero cells. Stock virus was prepared by 3× freezing and thawing and purified by sucrose gradient centrifugation. The same stock was used to infect mice by intraperitoneal (IP) injection with 5×10^4 plaque-forming units purified CVB3 3 months after induction with tamoxifen. We did not detect any background specific differences in virus infection, comparing the mixed 129SVJ/C57black6 and either parental strain (data not shown). Animals were killed at 10 or 28 days after injection with virus (p.i.); noninfected KO and Cre-negative animals were used as control subjects.

Tissue preparation. Samples of aseptically removed tissues were either fixed for 12 h in phosphate-buffered (pH 7.2) 4% paraformaldehyde and embedded in paraffin for histology, in situ hybridization, or quick-frozen in liquid nitrogen for subsequent preparation of ribonucleic acid (RNA) and protein.

Histopathology. Histological analysis was performed on deparaffinized 5-μm-thick tissue sections that were stained with hematoxylin and eosin to assess cellular injury and inflammation (18). Masson's Trichrome stain was used to visualize the degree of fibrosis. Immunohistochemistry was used to follow CVB3 infection with the VP1 antibody as published previously (19).

In situ hybridization and quantification of CVB3 infection. Localization of CVB3 RNA in paraffinated tissue sections was done by radioactive in situ hybridization. At the indicated time points, tissue samples were fixed in 4% paraformaldehyde/0.1 mol/l sodium phosphate buffer (pH 7.2) and embedded in paraffin for detection of viral RNA with a ^{35}S-labeled enterovirus-specific RNA probe as previously described (18). Tissue sections were exposed for 3 weeks and counterstained with hematoxylin and eosin. The detection of replication is a robust and sensitive method to document virus-infected cells. Lacking sensitive assays for virus entry in vivo and because CAR has never been implied in replication of CVB3, we used in situ hybridization to detect replication as a measure for virus entry dependent on CAR. To quantify the area fraction of infection, we used ImageJ version 14.1k (National Institutes of Health, Bethesda, Maryland) as outlined in the user manual.

Expression analysis. The RNA from heart, pancreas, spleen, gut, liver, lung, and kidney was isolated from individual mice and amplified with TaqMan probes for CAR, interleukin (IL)-6, IL-10, tumor necrosis factor (TNF)α, lymphocyte protein tyrosine kinase (LCK), interferon (IFN)γ CVB3, and glyceraldehyde-3-phosphate dehydrogenase (for normalization) as described previously (20). The probesets used are as follows: CAR-AGCTGCACGGTTCAAAACAGA (forward), TTCCGGCTCGGTTGGA (reverse), 6-FAM-CTCTGACCAGTGTATGCTGCGACTAGACGT-TAMRA (probe); IL-6-ACAAGTCGGAGGCTTAATTACACAT (forward), TTGCCATTGCACAACTCTTTTC (reverse), 6-FAM-TTCTCTGGGAAATCGTGGAAATG-TAMRA (probe, exon 2); IL-10-CCAGAGCCACATGCTCCTAGA (forward), GGTCCTTTGTTTGAAAGAAAGTCTTC (reverse), 6-FAM-CTGCGGACTGCCTTCAGCCAGG-TAMRA (probe); TNFα-CATCTTCTCAAAATTCGAGTGACAA (forward), CCAGCTGCTCCTCCACTTG (reverse), 6-FAM-CCTGTAGCCCACGTCGTAGCAAACCA-TAMRA (probe); IFNγ-CAGCAACAGCAAGGCGAAA (forward), CTGGACCTGTGGGTTGTTGAC (reverse), 6-FAM-AGGATGCATTCATGAGTATTGCCAAGTTTGA-TAMRA (probe); CVB3 (M16572)-CCCTGAATGCGGCTAATCC (forward), AAACACGGACACCCAAAGTAGTC (reverse), 6-FAM-CG-

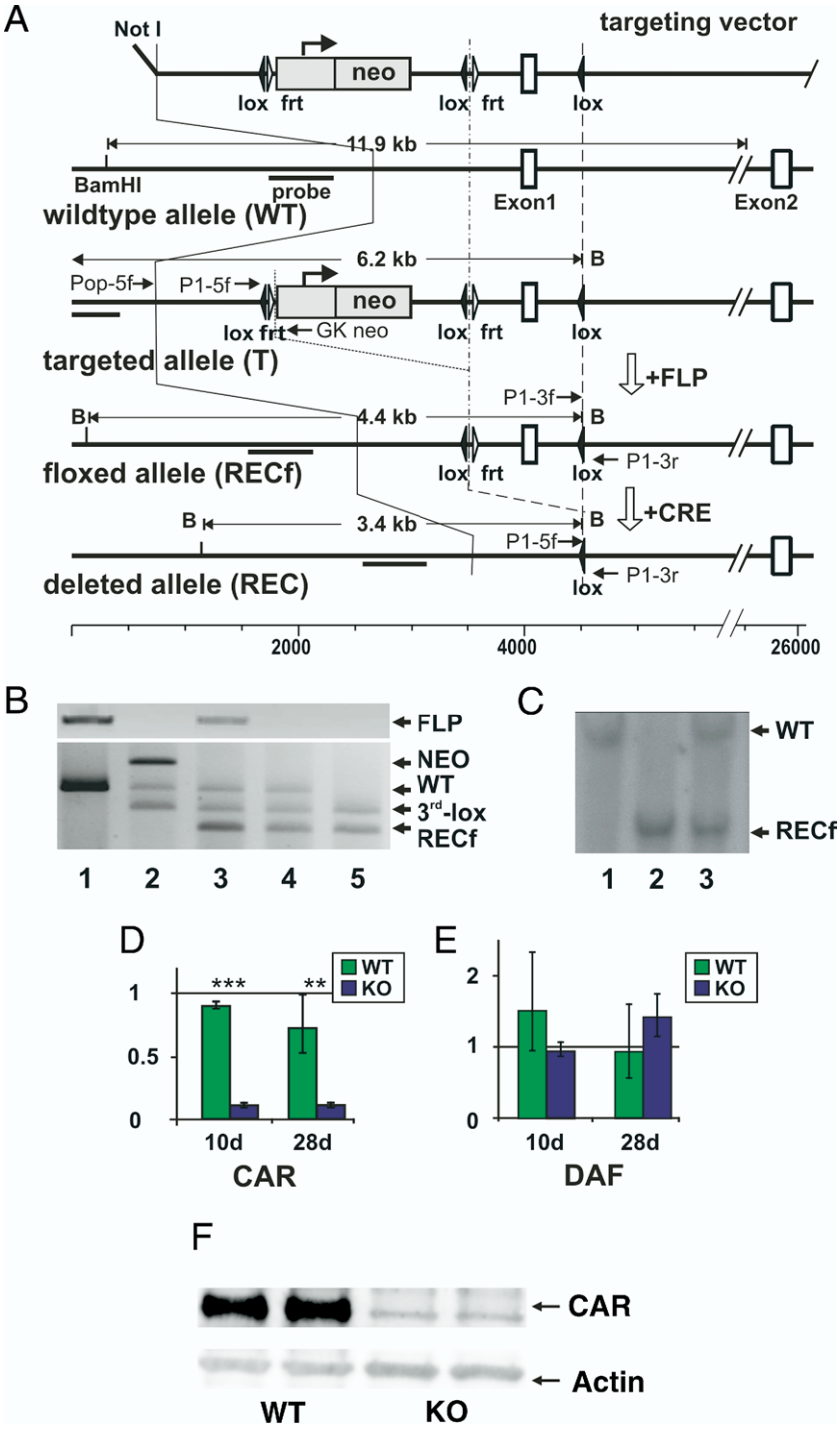

Figure 1 Tamoxifen Inducible Cardiac Specific CAR Knockout

(A) Targeting strategy: Exon 1, which contains the translation start is replaced with the floxed exon 1 and the flippase recognition target (FRT) flanked neo-cassette. The neo-cassette is subsequently removed through germline expression of the flippase (FLP) recombinase. **(B)** Polymerase chain reaction (PCR)-based genotyping with the primers indicated in **(A)** was used to detect the fragments corresponding to wild-type (WT), NEO, 3rd-lox, and RECf allele. The colony was established by mating FLP transgenics [1] to targeted animals [2]. The resulting double heterozygous animals [3] were used to obtain floxed heterozygous [4] and homozygous animals [5]. **(C)** For Southern blot genomic DNA was digested with BamHI, hybridized with a 600 bp PCR product (probe). The 12-kb WT allele and the 4.4-kb RECf allele were used to distinguish WT [1], knockout (KO) [2], and heterozygous animals [3]. Coxsackievirus-adenovirus receptor (CAR) ribonucleic acid **(D)** and protein levels **(F)** are altered with a strong effect in MerCreMer transgenic animals 3 months after the tamoxifen treatment, whereas the expression of the coreceptor decay-accelerating factor (DAF) was not significantly changed **(E)**; n = 3/group; **p ≤ 0.01; ***p ≤ 0.001.

CTGCAGAGTTGCCCGTTACGA-TAMRA (probe); glyceraldehyde-3-phosphate dehydrogenase-GGCAA-ATTCAACGGCACAGT (forward), AGATGGTG-ATGGGCTTCCC (reverse), 6-FAM-AGGCCGAG-AATGGGAAGCTTGTCATC-TAMRA (probe); LCK–CCTTCAACTTCGTGGCGAAA (forward), CG-TCCTTACGGCTCAGATTCTT (reverse), 6-FAM-AAACAGCCTGGAGCCTGAACCTTGG-TAMRA (probe). The DAF1 gene expression assay was purchased from Applied Biosystems (Foster City, California).

Protein was isolated by homogenization in liquid nitrogen and lysis in 8 mol/l urea, 4% CHAPS with DDT (80 mmol/l final) and protease inhibitor (PMSF). After electrophoresis on 12% sodium dodecyl sulfate polyacrylamide gel electrophoresis, samples were transferred to nitrocellulose-membrane Hybond-C extra (GE Healthcare, Piscataway, New Jersey). Membranes were blocked with 5% skim milk in phosphate-buffered saline–Tween 20 followed by incubation with commercial antibodies against CAR (rabbit polyclonal, Santa Cruz Biotechnology, Santa Cruz, California) and α-actin (mouse monoclonal, Sigma, St. Louis, Missouri) according to the manufacturer's instructions and detected with horseradish peroxidase-conjugated secondary antibodies and chemiluminescence staining with ECL (SuperSignal West Pico Chemiluminescent Substrate, Pierce, Rockford, Illinois).

Surgical procedures and hemodynamic measurements. The animals were anesthetized (thiopental 125 mg/kg IP), intubated, and artificially ventilated. As recently described, a 1.4-F microconductance pressure catheter (ARIA SPR-719, Millar-Instruments, Inc., Houston, Texas) was positioned in the left ventricle (LV) for continuous registration of LV pressure–volume loops in an open-chest as described previously in a closed-chest model (21). Calibration of the volume signal was obtained by hypertonic saline (10%) wash-in technique (22). Systolic function was quantified by LV end-systolic pressure (mm Hg) and dP/dt_{max} (mm Hg/s) as an index of LV contractility. Diastolic function was measured by LV end-diastolic pressure (mm Hg) and dP/dt_{min} (mm Hg/s). Global cardiac function was quantified by the end systolic and diastolic volume (μl), ejection fraction (% calculated), and heart rate (beats/min).

Statistical analysis. For statistical analysis, GraphPad Prism software (San Diego, California) was used. Results are expressed as mean ± SEM. For hemodynamic data statistical

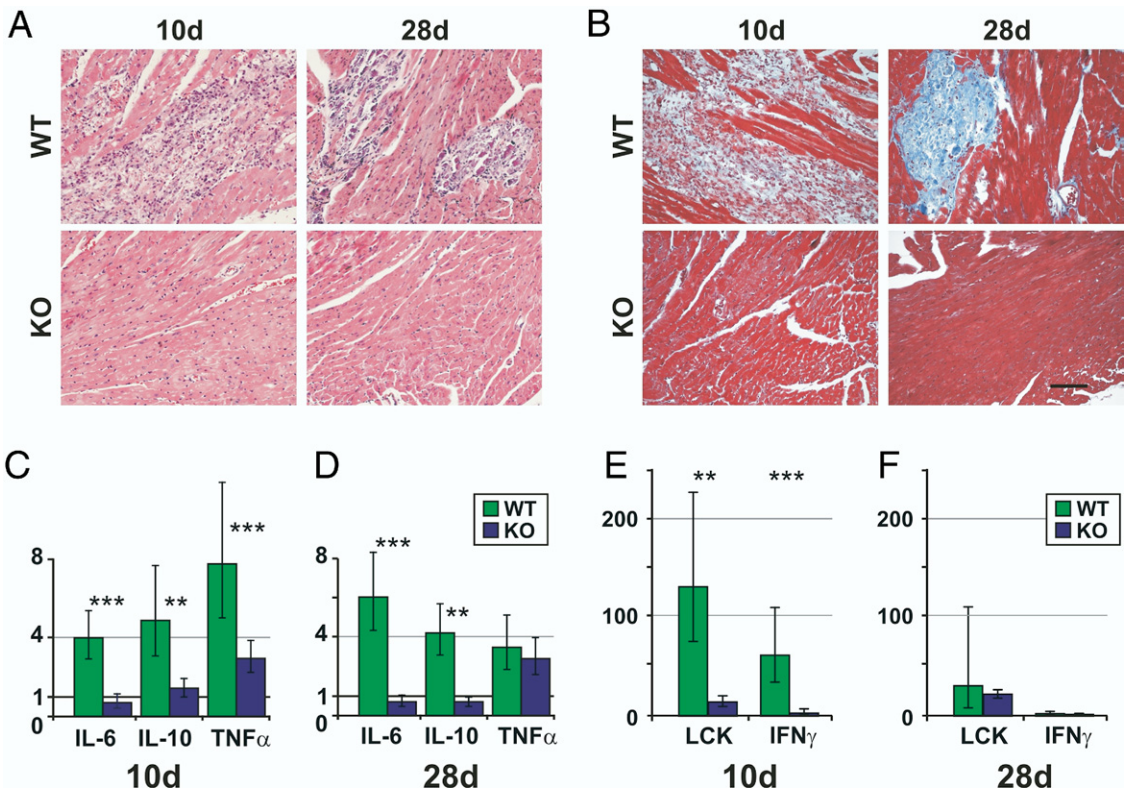

Figure 2 **Removal of CAR in Adult Cardiomyocytes Prevents Virus Uptake and Myocarditis**

(A) After infection with Coxsackievirus B3, WT animals show myocyte necrosis and inflammation with infiltration of mononuclear cells, which is not detectable in the CAR KO animals. **(B)** Trichrome staining reveals increased collagen deposition in areas of the cardiac lesion in WT animals but not in CAR KO mice. The fibrotic lesions solidify at day 28 after injection with virus (p.i.) in the heart of WT mice. Scale bar = 50 μm. **(C, D)** After 10 days or 28 days p.i., markers for inflammation such as interleukin (IL)-6, IL-10, and tumor necrosis factor (TNF)α were elevated in either genotype, with high levels in the WT animals. **(E, F)** Cardiac messenger ribonucleic acid levels of inflammation markers lymphocyte protein tyrosine kinase (LCK) and interferon (IFN)γ were >10× different between LCK and IFNγ; n = 36. **p ≤ 0.01; ***p ≤ 0.001. Abbreviations as in Figure 1.

significance between groups was determined with the Mann-Whitney *U* test; for expression analysis we used an unpaired 2-tailed *t* test. The significance level was chosen as $p = 0.05$.

Results

Cardiac CVB3 infection can be abolished by eliminating CAR. We used a conditional KO mouse (Fig. 1) to evaluate the role of CAR in CVB3-induced myocarditis in the adult heart. After 2 weeks of induction with tamoxifen, protein levels in the KO are <10% of WT levels (Fig. 1D). CVB3 readily infects cardiomyocytes in vitro and in vivo (17,18). In our experiments we used the CVB3 Nancy strain, which has been shown to depend on CAR for infection (4). In CVB3-infected WT mice we were able to detect myocyte necrosis and signs of inflammation as shown by infiltration of mononuclear inflammatory cells at day 10 after infection and subsequent fibrosis at day 28 (Figs. 2A and 2B). In contrast, the CAR-deficient KO hearts did not show any significant morphological changes. The protection of CAR-deficient hearts from myocarditis was also reflected by the cardiac messenger RNA levels of the cytokines IL-6, IL-10, TNFα, IFNγ, and the T-cell protein LCK with only minor elevations in the KO as compared with the marked increased in WT mice (Figs. 2C to 2F). To document that CAR efficiently blocks virus uptake into cardiomyocytes, we used in situ hybridization capable of detecting virus RNA and immunohistochemistry to visualize CVB3-VP1 protein in single infected cardiac cells. As shown in Figure 3, virus replication was detected in the heart, pancreas, and spleen, whereas small intestine, liver, lung, and kidney did not show signs of infection 10 days after IP infection with CVB3. We did not detect a single infected cardiomyocyte within 60 tissue sections derived from 20 KO hearts, which was unexpected. In contrast, virus entry and replication did not differ between genotypes in spleen or pancreas at day 10 p.i. (Fig.

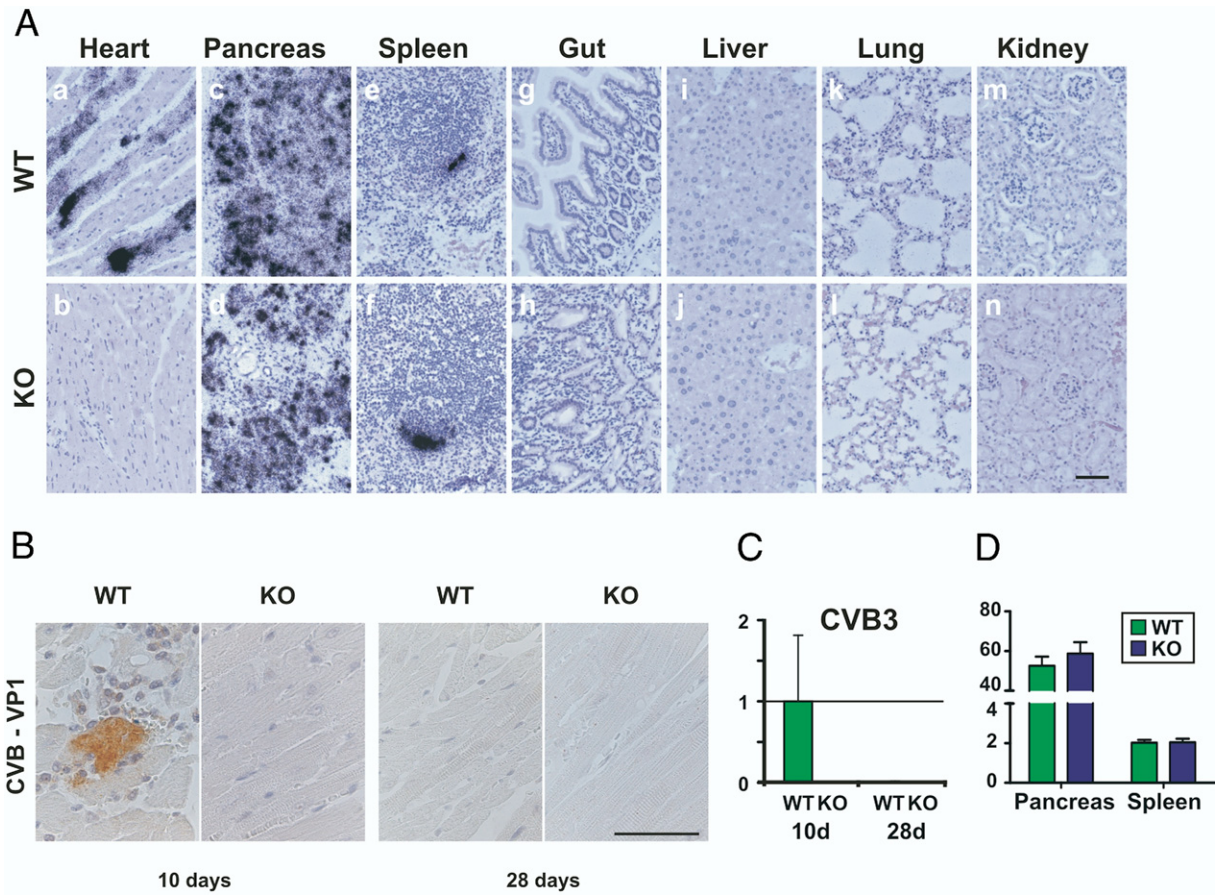

Figure 3 Virus Entry into the Heart Is Blocked After Deletion of CAR

(A) The distribution of replicating virus was visualized by in situ hybridization with a probe specific to Coxsackievirus B3 (CVB3). In the WT heart, approximately 30% of cardiomyocytes are infected at day 10 after injection with virus (p.i.) as indicated by the silver grain precipitates (dark signal) reflecting the virus ribonucleic acid (RNA) **(a)**, whereas not a single virus positive cell could be detected in KO hearts **(b)**. The extent of infection of other susceptible organs was similar in WT and KO mice **(c, e)** vs. **(d, f)**. Gut, liver, lung, and kidney were not infected in either KO or WT animals **(g to n)**. **(B)** Coxsackievirus protein was detected with an antibody directed against VP1 with focal expression in myocytes at 10 days after infection only in the WT heart. **(C)** Virus RNA was only present in the WT heart at day 10 as determined by Taq-Man analysis. Size bar = 50 μm. **(D)** Quantification of CVB3 infection in pancreas and spleen (n = 3/group). At day 10 p.i., the area fraction of infection in pancreas was 52.6% in WT and 58.7% in KO ($p = 0.36$) and in spleen was 2% independent of the genotype ($p = 0.87$). Abbreviations as in Figure 1.

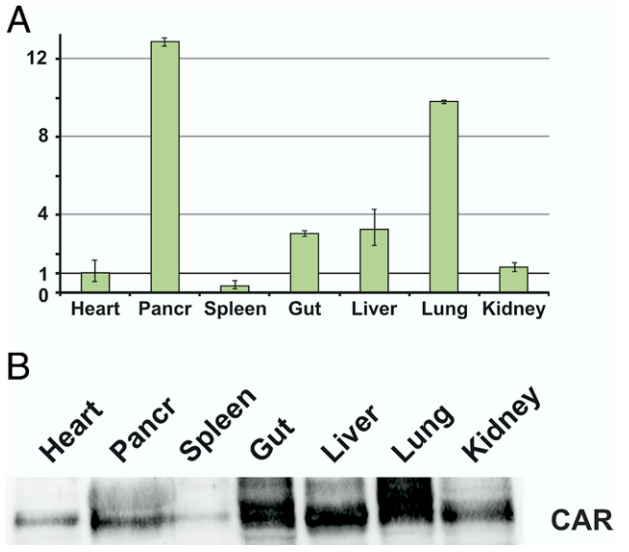

Figure 4 **Expression of CAR in the Adult Mouse Heart, Pancreas, Spleen, Gut, Liver, Lung, and Kidney (Wild-Type Males at 6 Months of Age)**

The Coxsackievirus-adenovirus receptor (CAR) messenger RNA **(A)** and protein levels **(B)** differ between tissues but do not correlate with infectivity of the tissue. Low levels of CAR expression are documented for adult heart, spleen, and kidney. The CAR messenger RNA levels differ >10× in pancreas (Pancr) and lung. The RNA levels are normalized to heart, n = 3. Increased protein expression was confirmed for pancreas, gut, liver, and lung.

3D) and was identical to our previous observation (23). Hence, in our inducible CAR-deficient mice only the heart was protected from virus entry and subsequent replication.

Factors other than CAR expression levels influence CVB3 distribution in target organs. To relate the distribution of virus infection RNA to CAR expression, we determined CAR messenger RNA and protein levels for all tissues tested (Figs. 4A and 4B). Not only did CAR expression levels differ by up to 25-fold between organs susceptible for virus infection (spleen vs. pancreas) but, conversely, tissues that were not susceptible such as gut, liver, and lung expressed CAR at levels that were 3- to 10-fold higher than cardiac expression.

Cardiac function after CVB3 infection. The functional consequences of CAR deficiency were evaluated by conductance catheter. Our results show that contractile function is maintained after CVB3 infection of CAR KO animals (Fig. 5). Whereas contractile function was impaired in control animals 10 days after infection (reduced contractility and ejection fraction and a trend to reduced developed pressure, cardiac output, and relaxation), CAR KO animals were unaffected. The maintenance of systolic (ejection fraction, P_{max}, dP/dt_{max}) and diastolic properties (dP/dt_{min} as a measure for active relaxation) in CVB3-infected KO hearts demonstrates that the elimination of CAR not only prevents structural changes but also preserves cardiac function after infection with CVB3.

Discussion

Viral myocarditis is one of the main causes of acute and chronic heart failure, and coxsackievirus is one of the important causative agents, which—especially in children—accounts for a significant fraction of cases of terminal heart failure (24). The disease process is mimicked in CVB3-infected mice with acute myocarditis that proceeds to a chronic phase that can ultimately lead to chronic cardiomyopathy (25). Here, we study the acute response to CVB3 in heart-specific CAR KO. To establish the animal model we infected a heart-specific tamoxifen-inducible KO with the cardiotropic CVB3 Nancy strain that has been described to produce severe myocarditis in mice (23).

CAR has not only been implicated in the progression of viral myocarditis on the basis of its function as a virus receptor, but various approaches to study CAR in vivo have indicated that reduced CAR expression or interference with CAR function could affect the disease process: CAR has been implicated in the early phases of myocarditis with reduced expression of CAR in MyD-88–deficient mice that are partially protected from CVB3-induced pathology (26). Although less of the virus was present in the MyD-88 KO cardiomyocytes, it is unclear whether this effect can be attributed to the reduced expression of CAR or to the concomitantly increased IFN-α. Soluble recombinant CAR has been used as an efficient tool to abolish CVB3-mediated myocarditis in mice, indicating the importance of the CAR–CVB3 interaction in the disease process (27). Whereas this approach is closer to the application as a therapeutic strategy, its effects can result from interaction of soluble CAR with the virus particle, endogenous CAR, or additional extracellular proteins. Here we decided to take a loss of function approach to exclusively investigate CAR in the acute phase of CVB3-induced myocarditis. With CAR expression reduced to 10% of WT levels, we were able to completely abolish cardiac pathology in the CVB3-infected KO mice (Fig. 2). Structural changes were absent as determined by histology, and not a single infected cardiomyocyte could be detected by in situ hybridization within a total of 20 investigated KO hearts (Fig. 3). As the MCM transgene directs expression of the recombinase exclusively to the heart, virus replication is retained in both pancreas and spleen of KO mice. This might help explain the increase in TNFα expression that—albeit reduced in the CVB3-infected CAR KO as compared to the CVB3-infected control heart—was 3-fold increased as compared with noninfected animals on the basis of cardiac RNA levels. Although CAR expression has been detected in multiple tissues including heart, brain, pancreas, liver, lung, and gut (9,28,29), the majority of those organs from WT mice did not show signs of virus infection (gut, liver, lung, and kidney). As confirmed on the RNA and protein level, these organs do express CAR, at levels that exceed cardiac expression in gut, liver, and lung that were nevertheless not infected. Failure of virus to enter these cells could derive from the spatial separation of virus and its receptor or the insufficient expression of coreceptors or intra-

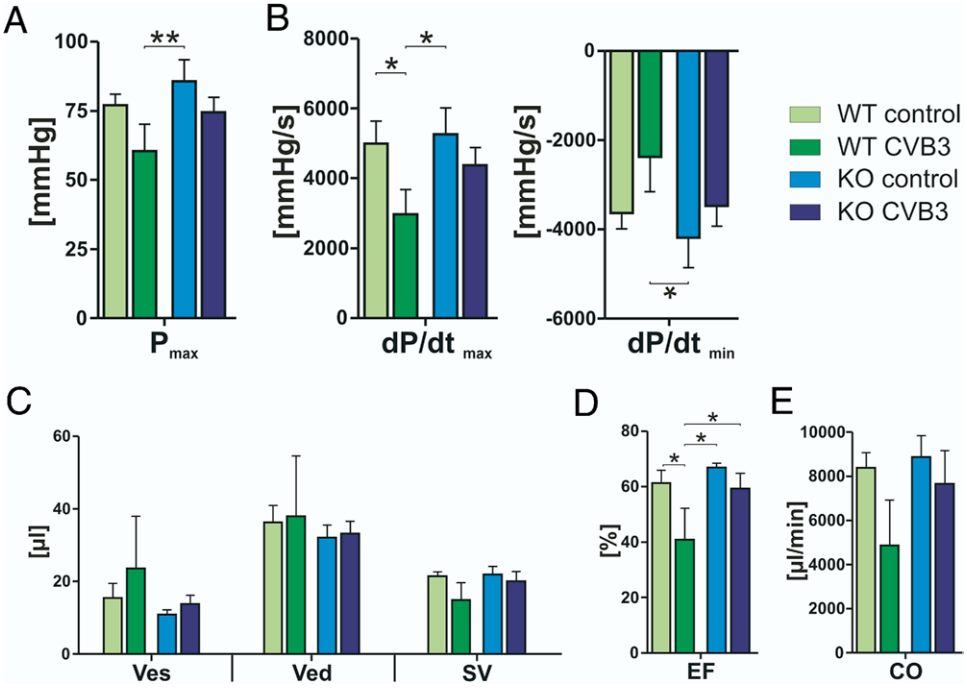

Figure 5 **Effect of CAR Deletion and CVB3 Infection on Cardiac Function**

Contractile function of Coxsackievirus B3 (CVB3)-infected WT hearts is reduced as compared with noninfected WT control animals unlike that of infected versus noninfected CAR KO animals. Statistical significance was obtained for contractility (dP/dt_{max}) **(B)** and ejection fraction **(D)**. In contrast, cardiac function is preserved in infected versus control KO animals **(dark bars in A to E)**. Animals were investigated 10 days after CVB3 infection; n = 30. *p ≤ 0.05; **p ≤ 0.01. CO = cardiac output; SV = stroke volume; Ved = end-diastolic volume; Ves = end-systolic volume; other abbreviations as in Figure 1.

cellular adaptor proteins, such as ZO1 and MUPP1 (4,5,7,30). Conversely, low levels of CAR expression as detected in the spleen do not preclude CVB3 infection. Unlike in the heart, where most cells are CAR-deficient, permissive cells in the spleen apparently do express CAR at sufficient levels to become infected. Overall, the tissue distribution and expression analysis indicate that CAR is necessary but not sufficient for virus entry in the mouse model of CVB3 infection. Its coreceptor DAF can by itself not mediate virus uptake as shown by Milstone et al. (31). There are DAF binding and nonbinding strains of CVB3, but even the DAF binding variant cannot mediate lytic infection without CAR (4). Thus, CAR exerts a dominant effect on virus entry that in the KO could not be overcome by DAF. In the CAR KO heart DAF expression was not significantly changed (Fig. 1E), indicating that it does not contribute to the phenotype.

To verify that CAR deficiency not only prevented morphological changes associated with myocarditis but also retained normal cardiac function, we analyzed the contractile and elastic properties of CVB3-infected and untreated KO and WT animals in vivo with the conductance catheter. In the acute phase CAR-deficient hearts were unaffected, whereas the CVB3-infected control hearts showed an impaired contractile function with a significant reduction in parameters of systolic function.

In addition to documenting the crucial role of CAR in virus entry into the heart in vivo, the established animal model provides novel insights into the pathogenesis of CVB-induced myocarditis. It has been argued that CVB myocarditis (at least, the chronic phase of disease) is autoimmune in nature. Because the MCM transgene is not expressed in T-cells, there is no reason to expect that putative autoreactive T-cells would not be induced in the conditional CAR KO. Here we show that virus infection of cardiomyocytes is a prerequisite for myocarditis and that—even as late as 28 days after infection—the KO-heart looks normal. All other susceptible organs can become infected and show the expected pathology in the CAR KO. This suggests a critical role for the productive infection of cardiomyocytes in the disease and argues against a primary autoimmune component in the pathogenesis.

So far, various therapeutic approaches to combat CVB3 infection have been proposed using CAR-transgenic erythrocytes to redirect and capture virus particles (32) or soluble CAR to compete with the cell surface receptor (27,33,34). Whereas the former has led to reduced lethality, the latter has worked in tissue culture (35) but produced inconsistent results in vivo, either ameliorating or aggravating the disease process in mice (27,33,34). On the basis of our findings, one could speculate that CAR indeed provides a suitable target

in the prevention and possible treatment of viral myocarditis, although future analysis will have to address potential unwanted effects that might be associated with the loss of CAR in the adult heart (36).

Acknowledgments

The authors thank Dr. Jeffrey Molkentin for the MCM transgenic mice and Beate Goldbrich, Mandy Terne, and Sandra Bundschuh for expert technical assistance.

Reprint requests and correspondence: Dr. Michael Gotthardt, Max-Delbrück-Center for Molecular Medicine Berlin-Buch, Robert-Rössle-Strasse 10, 13125 Berlin, Germany. E-mail: gotthardt@mdc-berlin.de; OR VCAPP, Washington State University, Wegner Hall, Room 205, Pullman, Washington 99164-6520. E-mail: gotthard@vetmed.wsu.edu.

REFERENCES

1. Bergelson JM, Cunningham JA, Droguett G, et al. Isolation of a common receptor for Coxsackie B viruses and adenoviruses 2 and 5. Science 1997;275:1320–3.
2. Tomko RP, Xu R, Philipson L. HCAR and MCAR: the human and mouse cellular receptors for subgroup C adenoviruses and group B coxsackieviruses. Proc Natl Acad Sci U S A 1997;94:3352–6.
3. Carson SD, Chapman NN, Tracy SM. Purification of the putative coxsackievirus B receptor from HeLa cells. Biochem Biophys Res Commun 1997;233:325–8.
4. Shafren DR, Williams DT, Barry RD. A decay-accelerating factor-binding strain of coxsackievirus B3 requires the coxsackievirus-adenovirus receptor protein to mediate lytic infection of rhabdomyosarcoma cells. J Virol 1997;71:9844–8.
5. Cohen CJ, Shieh JT, Pickles RJ, Okegawa T, Hsieh JT, Bergelson JM. The coxsackievirus and adenovirus receptor is a transmembrane component of the tight junction. Proc Natl Acad Sci U S A 2001;98:15191–6.
6. Sollerbrant K, Raschperger E, Mirza M, et al. The Coxsackievirus and adenovirus receptor (CAR) forms a complex with the PDZ domain-containing protein ligand-of-numb protein-X (LNX). J Biol Chem 2003;278:7439–44.
7. Coyne CB, Voelker T, Pichla SL, Bergelson JM. The coxsackievirus and adenovirus receptor interacts with the multi-PDZ domain protein-1 (MUPP-1) within the tight junction. J Biol Chem 2004; 279:48079–84.
8. Chung SK, Kim JY, Kim IB, Park SI, Paek KH, Nam JH. Internalization and trafficking mechanisms of coxsackievirus B3 in HeLa cells. Virology 2005;333:31–40.
9. Fechner H, Haack A, Wang H, et al. Expression of coxsackie adenovirus receptor and alphav-integrin does not correlate with adenovector targeting in vivo indicating anatomical vector barriers. Gene Ther 1999;6:1520–35.
10. Asher DR, Cerny AM, Weiler SR, et al. Coxsackievirus and adenovirus receptor is essential for cardiomyocyte development. Genesis 2005;42:77–85.
11. Dorner AA, Wegmann F, Butz S, et al. Coxsackievirus-adenovirus receptor (CAR) is essential for early embryonic cardiac development. J Cell Sci 2005;118:3509–21.
12. Chen JW, Zhou B, Yu QC, et al. Cardiomyocyte-specific deletion of the coxsackievirus and adenovirus receptor results in hyperplasia of the embryonic left ventricle and abnormalities of sinuatrial valves. Circ Res 2006;98:923–30.
13. Coyne CB, Bergelson JM. Virus-induced Abl and Fyn kinase signals permit coxsackievirus entry through epithelial tight junctions. Cell 2006;124:119–31.
14. Tracy S, Hofling K, Pirruccello S, Lane PH, Reyna SM, Gauntt CJ. Group B coxsackievirus myocarditis and pancreatitis: connection between viral virulence phenotypes in mice. J Med Virol 2000;62:70–81.
15. Gotthardt M, Hammer RE, Hubner N, et al. Conditional expression of mutant M-line titins results in cardiomyopathy with altered sarcomere structure. J Biol Chem 2003;278:6059–65.
16. Sohal DS, Nghiem M, Crackower MA, et al. Temporally regulated and tissue-specific gene manipulations in the adult and embryonic heart using a tamoxifen-inducible Cre protein. Circ Res 2001;89:20–5.
17. Kandolf R, Hofschneider PH. Molecular cloning of the genome of a cardiotropic Coxsackie B3 virus: full-length reverse-transcribed recombinant cDNA generates infectious virus in mammalian cells. Proc Natl Acad Sci U S A 1985;82:4818–22.
18. Klingel K, Hohenadl C, Canu A, et al. Ongoing enterovirus-induced myocarditis is associated with persistent heart muscle infection: quantitative analysis of virus replication, tissue damage, and inflammation. Proc Natl Acad Sci U S A 1992;89:314–8.
19. Werner S, Klump WM, Schonke H, Hofschneider PH, Kandolf R. Expression of coxsackievirus B3 capsid proteins in Escherichia coli and generation of virus-specific antisera. DNA 1988;7:307–16.
20. Weinert S, Bergmann N, Luo X, Erdmann B, Gotthardt M. M line-deficient titin causes cardiac lethality through impaired maturation of the sarcomere. J Cell Biol 2006;173:559–70.
21. Westermann D, Rutschow S, Jager S, et al. Contributions of inflammation and cardiac matrix metalloproteinase activity to cardiac failure in diabetic cardiomyopathy: the role of angiotensin type 1 receptor antagonism. Diabetes 2007;56:641–6.
22. Steendijk P, Staal E, Jukema JW, Baan J. Hypertonic saline method accurately determines parallel conductance for dual-field conductance catheter. Am J Physiol Heart Circ Physiol 2001;281:H755–63.
23. Klingel K, Stephan S, Sauter M, et al. Pathogenesis of murine enterovirus myocarditis: virus dissemination and immune cell targets. J Virol 1996;70:8888–95.
24. Feldman AM, McNamara D. Myocarditis. N Engl J Med 2000;343: 1388–98.
25. Fairweather D, Rose NR. Coxsackievirus-induced myocarditis in mice: a model of autoimmune disease for studying immunotoxicity. Methods 2007;41:118–22.
26. Fuse K, Chan G, Liu Y, et al. Myeloid differentiation factor-88 plays a crucial role in the pathogenesis of Coxsackievirus B3-induced myocarditis and influences type I interferon production. Circulation 2005;112:2276–85.
27. Yanagawa B, Spiller OB, Proctor DG, et al. Soluble recombinant coxsackievirus and adenovirus receptor abrogates coxsackievirus b3-mediated pancreatitis and myocarditis in mice. J Infect Dis 2004;189: 1431–9.
28. Bergelson JM, Krithivas A, Celi L, et al. The murine CAR homolog is a receptor for coxsackie B viruses and adenoviruses. J Virol 1998;72:415–9.
29. Tomko RP, Johansson CB, Totrov M, Abagyan R, Frisen J, Philipson L. Expression of the adenovirus receptor and its interaction with the fiber knob. Exp Cell Res 2000;255:47–55.
30. Cohen CJ, Gaetz J, Ohman T, Bergelson JM. Multiple regions within the coxsackievirus and adenovirus receptor cytoplasmic domain are required for basolateral sorting. J Biol Chem 2001;276:25392–8.
31. Milstone AM, Petrella J, Sanchez MD, Mahmud M, Whitbeck JC, Bergelson JM. Interaction with coxsackievirus and adenovirus receptor, but not with decay-accelerating factor (DAF), induces A-particle formation in a DAF-binding coxsackievirus B3 isolate. J Virol 2005;79:655–60.
32. Asher DR, Cerny AM, Finberg RW. The erythrocyte viral trap: transgenic expression of viral receptor on erythrocytes attenuates coxsackievirus B infection. Proc Natl Acad Sci U S A 2005; 102:12897–902.
33. Dorner A, Grunert HP, Lindig V, et al. Treatment of coxsackievirus-B3-infected BALB/c mice with the soluble coxsackie adenovirus receptor CAR4/7 aggravates cardiac injury. J Mol Med 2006;84:842–51.
34. Lim BK, Choi JH, Nam JH, et al. Virus receptor trap neutralizes coxsackievirus in experimental murine viral myocarditis. Cardiovasc Res 2006;71:517–26.
35. Goodfellow IG, Evans DJ, Blom AM, et al. Inhibition of coxsackie B virus infection by soluble forms of its receptors: binding affinities, altered particle formation, and competition with cellular receptors. J Virol 2005;79:12016–24.
36. Lim BK, Xiong D, Dorner A, et al. Coxsackievirus and adenovirus receptor (CAR) mediates atrioventricular-node function and connexin 45 localization in the murine heart. J Clin Invest 2008;118:2758–70.

Key Words: cell adhesion molecules ■ myocarditis ■ receptors ■ viruses.